EUMETSAT Satellite Application Facility on Climate Monitoring

Algorithm Theoretical Baseline Document

Joint Cloud property Histogram products
AVHRR

Joint Cloud property Histogram   **CM-11025**

Document Signature Table

	Name	Function	Signature	Date
Author	Joseph Sedlar Karl-Göran Karlsson Jan Fokke Meirink Nikos Benas	CM SAF scientists		27/05/2016 19/08/2016 15/10/2020
Editor	Rainer Hollmann	Science Coordinator		15/10/2020
Approval	Steering Group			
Release	Martin Werscheck	CM SAF Manager		

Distribution List

Internal Distribution	
Name	**No. Copies**
DWD Archive	1
CM SAF Team	1

External Distribution		
Company	**Name**	**No. Copies**
PUBLIC		

Document Change Record

Issue/ Revision	Date	DCN No.	Changed Pages/Paragraphs
1.0	15/10/2020	SAF/CM/SMHI/ATBD/GAC/JCH	Initial release, split of existing ATBD JCH (RD-1) into a specific document for CLARA A2.1

Applicable documents

Reference	Title	Code
AD 1	CM SAF Product Requirement Document	SAF/CM/DWD/PRD/3.5

Reference documents

Reference	Title	Code
RD 2	Algorithm Theoretical Baseline Document: Joint Cloud property Histogram products AVHRR/SEVIRI	SAF/CM/SMHI/ATBD/JCH/2.2

![EUMETSAT CM SAF CLIMATE MONITORING]	**Algorithm Theoretical Baseline Document Joint Cloud property Histogram products**	Doc.No.: SAF/CM/SMHI/ATBD/GAC/JCH Issue: 1.0 Date: 15.10.2020

TABLE of CONTENT

LIST of FIGURES

1 The EUMETSAT SAF on Climate Monitoring

The importance of climate monitoring with satellites was recognized in 2000 by EUMETSAT Member States when they amended the EUMETSAT Convention to affirm that the EUMETSAT mandate is also to "contribute to the operational monitoring of the climate and the detection of global climatic changes". Following this, EUMETSAT established within its Satellite Application Facility (SAF) network a dedicated centre, the SAF on Climate Monitoring (CM SAF, http://www.cmsaf.eu).

The consortium of CM SAF currently comprises the Deutscher Wetterdienst (DWD) as host institute, and the partners from the Royal Meteorological Institute of Belgium (RMIB), the Finnish Meteorological Institute (FMI), the Royal Meteorological Institute of the Netherlands (KNMI), the Swedish Meteorological and Hydrological Institute (SMHI), the Meteorological Service of Switzerland (MeteoSwiss), and the Meteorological Service of the United Kingdom (UK MetOffice). Since the beginning in 1999 , the EUMETSAT Satellite Application Facility on Climate Monitoring (CM SAF) has developed and will continue to develop capabilities for a sustained generation and provision of Climate Data Records (CDR's) derived from operational meteorological satellites.

In particular the generation of long-term data records is pursued. The ultimate aim is to make the resulting data records suitable for the analysis of climate variability and potentially the detection of climate trends. CM SAF works in close collaboration with the EUMETSAT Central Facility and liaises with other satellite operators to advance the availability, quality and usability of Fundamental Climate Data Records (FCDRs) as defined by the Global Climate Observing System (GCOS). As a major task the CM SAF utilizes FCDRs to produce records of Essential Climate Variables (ECVs) as defined by GCOS. Thematically, the focus of CM SAF is on ECVs associated with the global energy and water cycle.

Another essential task of CM SAF is to produce data records that can serve applications related to the new Global Framework of Climate Services initiated by the WMO World Climate Conference-3 in 2009. CM SAF is supporting climate services at national meteorological and hydrological services (NMHSs) with long-term data records but also with data records produced close to real time that can be used to prepare monthly/annual updates of the state of the climate. Both types of products together allow for a consistent description of mean values, anomalies, variability and potential trends for the chosen ECVs. CM SAF ECV data records also serve the improvement of climate models both at global and regional scale.

As an essential partner in the related international frameworks, in particular WMO SCOPE-CM (Sustained COordinated Processing of Environmental satellite data for Climate Monitoring), the CM SAF - together with the EUMETSAT Central Facility, assumes the role as main implementer of EUMETSAT's commitments in support to global climate monitoring. This is achieved through:

- Application of highest standards and guidelines as lined out by GCOS for the satellite data processing,

- Processing of satellite data within a true international collaboration benefiting from developments at international level and pollinating the partnership with own ideas and standards,

- Intensive validation and improvement of the CM SAF climate data records,

- Taking a major role in data record assessments performed by research organisations such as WCRP. This role provides the CM SAF with deep contacts to research organizations that form a substantial user group for the CM SAF CDRs,

- Maintaining and providing an operational and sustained infrastructure that can serve the community within the transition of mature CDR products from the research community into operational environments.

A catalogue of all available CM SAF products is accessible via the CM SAF webpage, www.cmsaf.eu/. Here, detailed information about product ordering, add-on tools, sample programs and documentation is provided.

2 Introduction

This CM SAF Algorithm Theoretical Baseline Document (ATBD) provides detailed information on the cloud Joint Cloud property Histogram (JCH) product. The JCH is delivered as a level-3 product of the 2nd editions of the **CM SAF** c**L**oud, **A**lbedo and **RA**diation data record from AVHRR-equipped satellite platforms (CLARA-A2.1) and **CM SAF** c**L**oud d**A**t**A**set using **S**EVIRI (CLAAS-2.1).

The JCH product is meant to facilitate direct, quantitative comparisons across the parameter space of multiple derived, and/or retrieved, CLARA-A2.1 and CLAAS-2.1 cloud parameters. The parameter space includes cloud fraction (CF), cloud top pressure (CTP), cloud top optical thickness (COT) and cloud phase (CPH). Traditionally, the most common display method of JCH data highlights the absolute or relative CF as a function of COT and CTP, for a specific CPH; an example of the parameter distribution space from ISCCP-D1 (Rossow and Schiffer, 1999) is shown in Figure 1. Detailed descriptions of the algorithm methodology and production of JCHs are provided in Section 3.
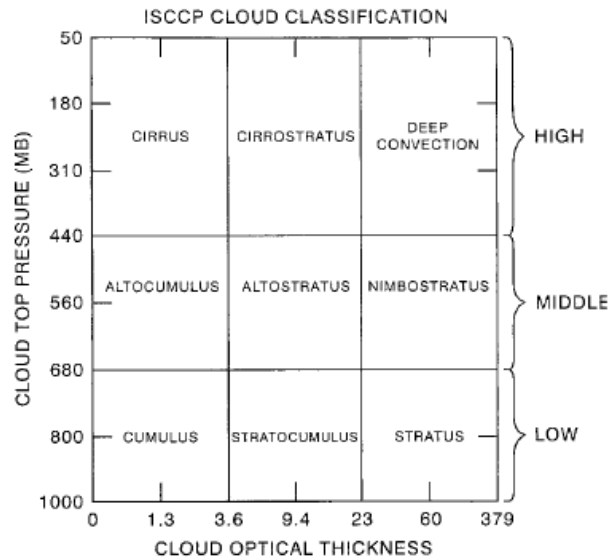
Figure 1: *Example ISCCP cloud classifications, highlighting defined CTP-COT parameter space bins. Cloud type and level classifications based on CTP [hPa] and COT developed for the ISCCP cloud type, taken from Rossow and Schiffer (1999).*

Advantages of subsampling data using the JCH framework were identified and developed during the initial ISCCP-D1 retrieval and archiving of cloud properties. Initially the motivation to produce JCH from ISCCP data was to manage data volume size (Rossow and Schiffer, 1991). However the authors quickly identified a closely inter-related behaviour between COT and CTP (cloud top height) (Rossow and Schiffer, 1991; 1999). The strong relationship between COT and CTP was used to identify distinct cloud regimes, or so-called "weather states", across the tropics (Rossow et al., 2005), as well as the subtropics and midlatitudes (Oreopoulos and Rossow, 2011). Likewise, comparisons of JCHs from multiple satellite data records have led to an improved understanding on advantages and disadvantages of satellite-derived cloud product retrieval algorithms (e.g., Marchand et al., 2010). Beyond observational studies on cloud characteristics, the JCH approach has been applied to evaluation of cloud properties from global climate model simulations (e.g., Lin and Zhang, 2004; Zhang et al.,

2005; Pincus et al., 2012), and also as a framework for examining cloud feedbacks relative to climate forcings (e.g., Zelinka et al., 2012).

The JCH product was released by CM SAF for the first time as a L3 product within the 1st processing versions of CLARA-A1 and CLAAS-1.

3 Joint Cloud property Histogram Algorithm description

3.1 Theoretical basis for the joint histogram approach

Construction of the JCH requires no additional product development; rather it is a post-processed statistical distribution consisting of a 4 dimensional cloud product parameter space. The cloud products consist of cloud mask (CMA), cloud top (CTO) and cloud phase (CPH) and cloud water path (CWP). The JCH product provides absolute frequency counts (integer) of the number of level-2 (CLAAS) or level-2b (CLARA) data products on a downscaled, equal-angle grid of 1° for CLARA and 0.25° for CLAAS, that are bounded by specified cloud optical thickness (COT) and cloud top pressure (CTP) bin ranges (see Figure 1). Counts are stored separately for liquid-determined and ice-determined cloud tops from the CPH product. A cloud fraction (%) is provided for each 1° by 1° grid point. This cloud fraction is different from the level-2 CMA and level-3 cloud fraction (CFC), and will be described below. Based on the integer counts and cloud fraction, it is possible to fully reconstruct the absolute and relative cloud fractions of total, liquid-only or ice-only clouds, as well as calculate the relative and absolute frequencies of cloud fraction within desired COT or CTP ranges. Details on the methods to recover absolute and relative statistics, and suggestions of potential usages of JCH data records, are provided in Section 4.

3.2 Methodology

CMA, CTO, CPH and CWP L2 products are provided twice daily (ascending and descending orbits) for each CLARA-A2.1 satellite in orbit for any given day on an equal angle grid resolution of 0.05°, while the same cloud products are provided for 96 time slots per day (15 minute temporal resolution) for CLAAS-2.1. These represent the input product variables for the construction of the JCH. The final JCH product is stored as a monthly product, individually for each satellite in orbit, as well as a concatenation of all available satellites in orbit for a particular month and year. The amount of input data into the histogram is thus a function of the time period within the CLARA-A2.1 data record (fewer satellites in orbit early in the record compared to later), as well as the number of cloudy grids with retrieved COT, CTP and CPH values. Only daytime observations are included in the JCH distributions since CWP products (including COT) can only be determined during daytime. In practice, the JCHs contain absolute counts for L2B/L2 observations at solar zenith angle smaller than 75°.

Processing of the JCH product adheres to the following algorithm qualitative logic:

1) A 0.25° by 0.25° (CLAAS) or 1° by 1° (CLARA) equal-angle grid is developed (JCH spatial grid)

2) COT and CTP statistical bins are strategically defined following guidance from the ISCCP JCH bin distributions (Rossow and Schiffer, 1991; 1999; Hahn et al., 2001). CLARA-A2.1 and CLAAS-2.1 JCHs consist of 15 CTP and 13 COT bins, with bin borders defined as:

CTP (hPa): [1, 90, 180, 245, 310, 375, 440, 500, 560, 620, 680, 740, 800, 875, 950, 1100]

COT: [0, 0.3, 0.6, 1.3, 2.2, 3.6, 5.8, 9.4, 15.0, 23.0, 41.0, 60.0, 80.0, 100.0]

3) At each point on the JCH spatial grid, the number (N) of L2B/L2 observations with a valid CMA, CTP and COT for each 15x13 CTP-COT JCH parameter space bin is recorded (integers); N is recorded separately for liquid and ice clouds (CPH). Quantatively, this follows

$$JCH(CPH, CTPbin, COTbin, lat, lon) = N(lat,lon)_{CTP \in CTPbin;\ COT \in COTbin;\ CPH \in liq|ice} \quad (1)$$

4) A total cloud fraction (CFC) for each JCH spatial grid point is computed. CFC is defined as:

$$CFC(lat,lon) = \frac{\sum JCH(1...n_{CPH}, 1...n_{CTP}, 1...n_{COT}, lat, lon)}{N_{TOT}(lat,lon) = N(lat,lon)_{cloudy} + N(lat,lon)_{clear}} \quad (2)$$

representing the total fraction of JCH counts normalized to the number of cloudy and cloud free L2B/L2 observations at a particular grid point. Note that CFC is not equivalent to cloud fraction calculated from the CMA for L2B or L2 observations because the CFC provided in the JCH data record requires a valid CTP and COT measure. Furthermore, the number of observations is reduced further by limiting observations to a maximum solar zenith angle of 75°.

Using the JCH binned counts and total grid CFC, Eq. (2) can be rearranged to solve for N_{TOT} for each JCH spatial grid. Calculation of N_{TOT} allows the user to calculate absolute and relative frequencies of cloud property distributions from the 4-dimensional parameter space of the JCH. Examples of how the JCH data can be applied are shown in the following section.

4 Applications of JCHs

JCHs provide a convenient approach to analyzing satellite-derived cloud properties across a multiple parameter space. Rossow and Schiffer (1991; 1999), Hahn et al. (2001) and Rossow et al. (2005) illustrate a well-documented relationship between CTP and COT. This relationship is based on the unique characteristics of different cloud types (e.g., stratiform, cumuliform) and their optical and vertical characteristic distributions. In this section we present an introductory glimpse at the information content included in the JCH post-processed data product. Data examples from global and tropical (20S-20N) JCHs processed in the latest release of the CLARA-A2.1 cloud climatological data record are presented in Section 4.1. An example of JCH from CLAAS-2.1 is given in Section 4.2.

4.1 Examples of JCH from CLARA-A2.1

Figures 2a-b show the spatial distribution of total (liquid and ice) cloud fraction reported with all JCHs for 1982-2014, concatenated for the months of January (a) and June (b). Note that the JCH CFC is only reported for daytime viewing observations when solar zenith angle is smaller than 75°; this effectively eliminates regions poleward of 50-60°, depending on season. These traditional spatial projections provide a wealth of information regarding the climatological distribution of clouds, in particular: relative minima in the subtropical subsidence

regions, the radiatively important stratocumulus regions, high cloud fractions in the North Pacific, North Atlantic storm track region and Southern Ocean, as well as the reduction in cloud occurrence over land relative to over ocean.
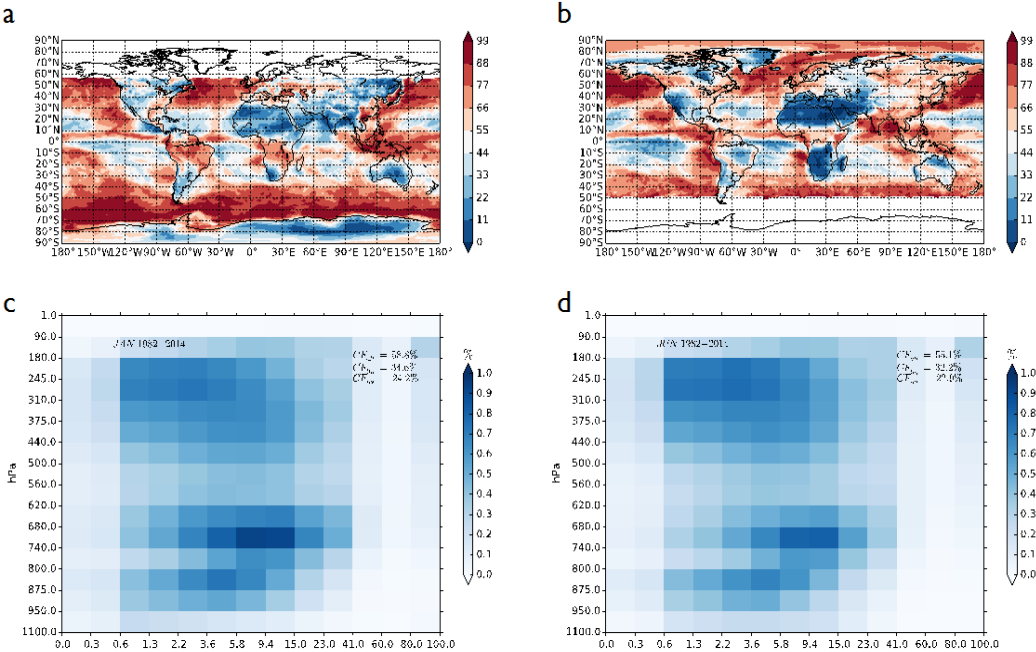

Figure 2: *Spatial distribution of mean total cloud fraction for 1982-2014 for January (a) and June (b) and corresponding two-dimensional plots of cloud occurrences (i.e., contribution to the total cloud fraction) in cloud top pressure and cloud optical thickness bins (c and d). JCHs are global between 60°S and 60°N.*

To include additional cloud characteristics such as cloud top pressure or optical thickness, two additional spatial plots are required. In Figure 2c-d, both of these cloud characteristics, in addition to cloud fraction, are included in a single JCH figure. The distributions are qualitatively similar for both boreal winter and summer months, with a peak cloud distribution in the mid troposphere (approx. 700 hPa) and cloud optical thicknesses primarily ranging 3.6-15. Despite similar peak distributions, there are some more subtle differences between these seasons. Total cloud fraction is slightly larger during January, and there is a slight increase (decrease) in mid-level clouds (upper-level clouds) spanning all optical thicknesses in January relative to June. These differences are more easily identifiable by calculating the absolute histogram differences for June from January months during 1982-2014 (Figure 3a).
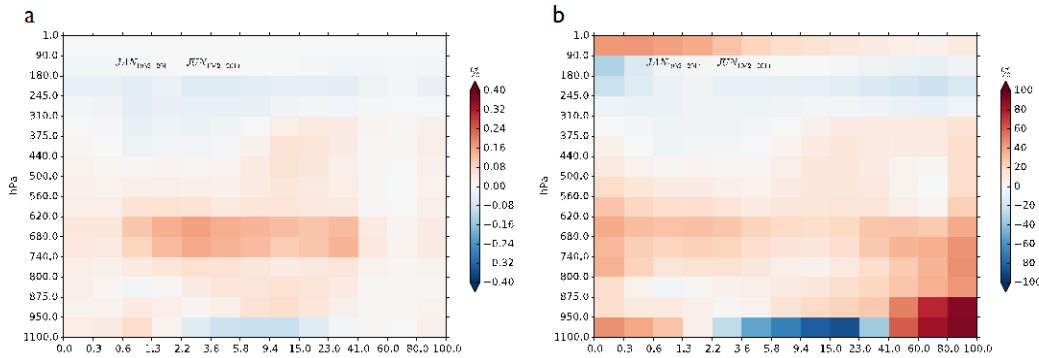
Figure 3: *Absolute (a) and relative (b) changes in global cloud frequency distributions between January and June in the period 1982-2014 between 60°S and 60°N (see Figure 2).*

Cloud analysis applications may benefit from examining the relative frequency distribution changes in the JCH distributions. Figure 3b shows the change in JCH distribution for January minus June, relative to the January distribution. Clearly the large relative changes between the months for the lowest-level clouds indicate a robust change in cloud distribution between January and June (Figure 3b), even though the absolute differences are relatively small (Figure 3a). Thus the distribution of cloud properties within JCHs can be manipulated in several ways to study varying aspects of cloud distribution climatologies.

To further illustrate potential uses of JCHs, we focus on cloud distributions within the tropics (20°S-20°N) during July 2010-2014 for two different satellite platforms, METOP-A and NOAA19. These two platforms are chosen since they have overlapping observation records with relatively little orbital drift, yielding rather stable equator crossing times (ECT) during the 5 year period. METOP-A has an ascending ECT at 09:30 UTC, while NOAA19 crosses at 13:30UTC. The purpose of these examples is to highlight how JCHs may provide insight on the impact of diurnal cycle (observation time) on cloud properties. Total (liquid and ice) JCHs are shown in Figure 4; panels a-b are for METOP-A and c-d for NOAA19, and include cumulative frequency distribution lines of absolute total, liquid-only and ice-only cloud fraction across the optical thickness (left panels) and cloud top pressure (right panels) bins.
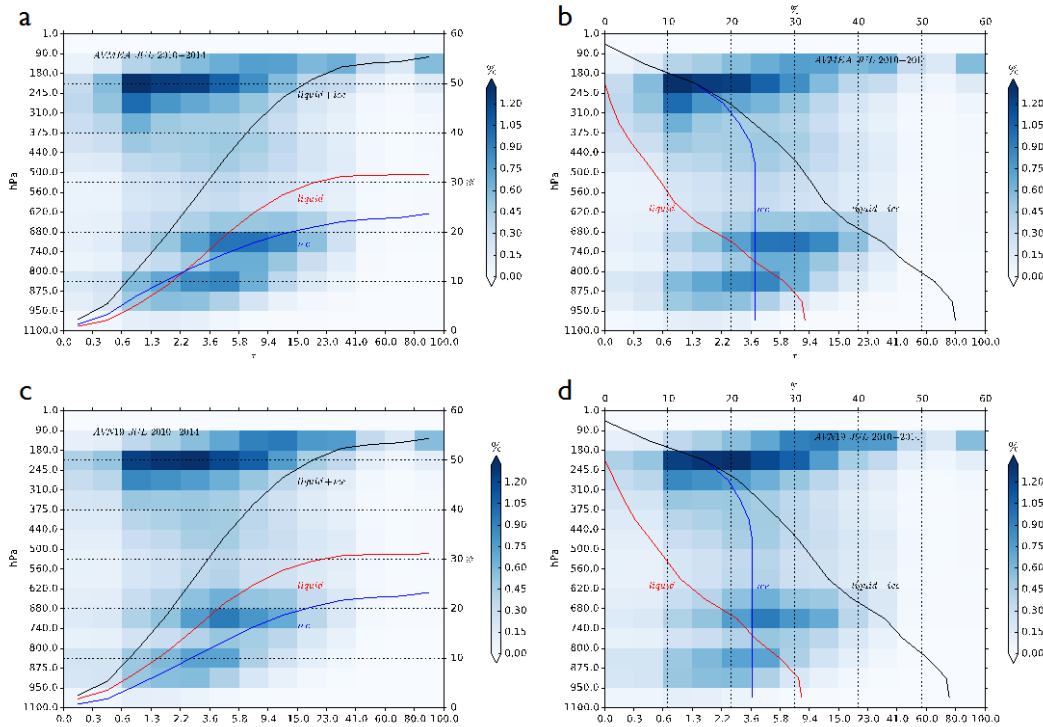
Figure 4: *JCH distributions in the tropical region (20°S-20°N) during July 2010-2014 for two different satellite platforms, METOP-A (a-b) and NOAA19 (c-d). Upper panels show the METOP-A morning observation near 10 am while lower panels show afternoon observations near 13:30 pm. Results are shown together with two alternative accumulative curves for liquid, ice and total cloud fraction (see text for explanation).*

The qualitative JCH distributions for the morning (METOP-A, upper panels) and afternoon (NOAA19, lower panels) overpasses are generally similar. The region is characterized by a relatively high frequency of upper-level (CTP < 350 hPa) cirrus clouds composed of ice (Figure 4b,d) with optical thickness generally below 3.6 (Figure 4a,c). Furthermore, low- to mid-level liquid clouds with an optical thickness range of 0.6 to 15, generally with increasing COT with height, are observed during both diurnal observations cycles. Absolute cloud fractions for total, liquid-only and ice-only are very similar for this region, regardless of observation time (see cloud fraction cumulative frequencies in Figure 4). The vertical distributions, however, indicate a slightly higher frequency of optically thin, high ice clouds in the morning overpasses.

The subtle differences in tropical cloud properties can be further scrutinized by examining JCHs over land and sea scenes separately (Figure 5). Highest total cloud fractions are observed over the sea compared to over land (fractions in upper right of each panel), where high-level cirrus are supported from vertical heat and moisture transport and detrainment due to convective systems. High-level cirrus and deep convective clouds are relatively more frequent during in the afternoon overpasses (Figure 5c) compared with morning (Figure 5a). However, low-level stratocumulus and shallow cumulus clouds show a general reduction in their occurrence frequencies transitioning from morning to afternoon (Figure 5a, c), indicative of a diurnal reduction in cloud occurrence with increased solar heating and absorption (solar zenith angle changes).
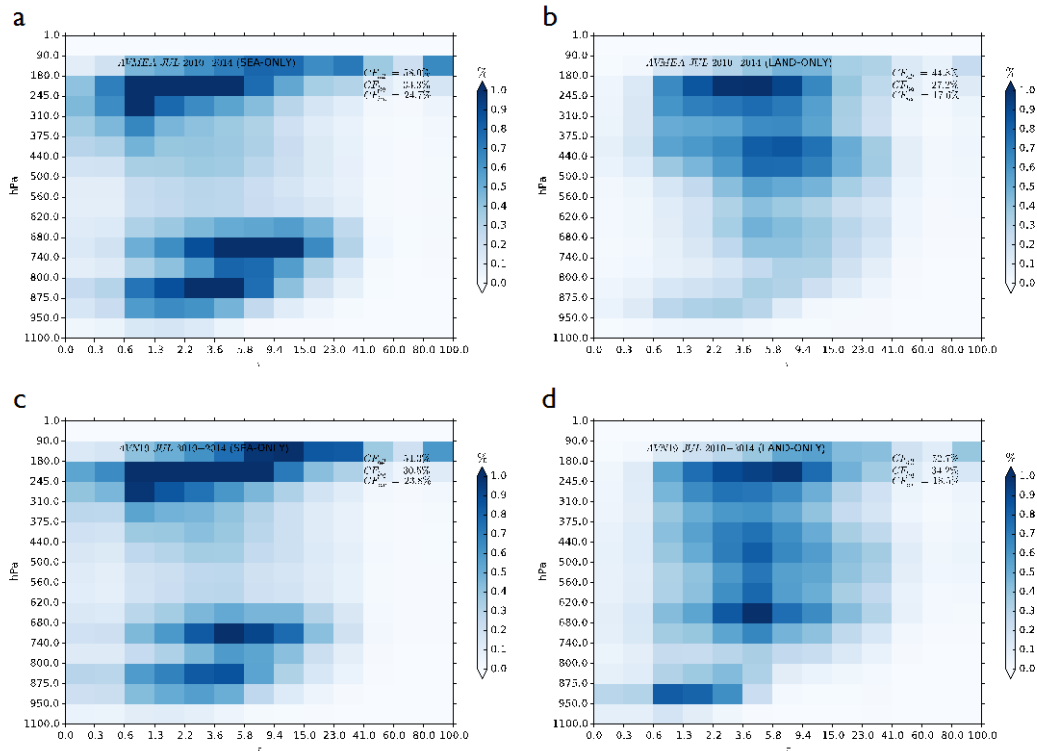
Figure 5: *Same as Figure 4 but separated into ocean (left) and land (right) contributions.*

Over land the cloud fraction is higher in the afternoon. Relative to morning, the afternoon has an 18% increase in cloud fraction (7% increase in liquid cloud fraction). This is more clearly evident in the increase shallow cumulus and mid-level altostratiform cloud layers. Upper level cloud distributions are similar.

4.2 Example of JCH from CLAAS-2.1 (SEVIRI)

An example of a COT/CTP-histogram for CLAAS-2.1 SEVIRI is given in Figure 6a. The histogram was created using data from the 45° S-N, W-E area of the SEVIRI disc for July 2010, with 0.25° × 0.25° spatial resolution. In this month, two major cloud clusters are found, namely low clouds with medium optical thickness (most cases in the range 2.2-15) and high clouds with lower optical thickness values (more often in the range 1.3-5.8). Low clouds occur in this region more often than high clouds, while an even less frequent occurrence of middle clouds is also discernible. While the distribution in COT space is broad for low clouds, the majority of them is located in only two pixels in CTP space, namely between 950 and 800 hPa.

Two pixels in the histogram of Figure 6a are highlighted with a yellow and an orange square, corresponding to the most frequent occurrences of high and low clouds, respectively. The absolute number of occurrences of clouds with properties bordered by CTP and COT, as indicated by these boxes, is shown in Figure 6b and c. For July 2010 low medium thick clouds are most often detected by SEVIRI in the Atlantic west of southern Africa, and secondarily west of northern Africa, while high medium thick clouds occur mainly in the ITCZ band, north of the equator.
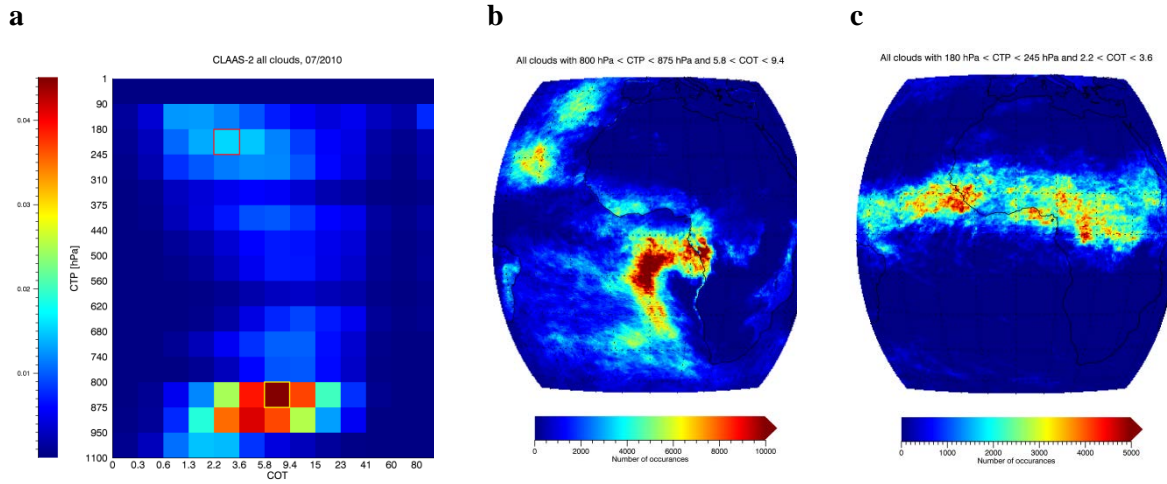
a

b

c

Figure 6: *(a) Joint histogram of CLAAS-2.1 COT and CTP for July 2010, using data aggregated from the complete SEVIRI disc; (b) Absolute number of occurrences of clouds with CTP between 800 hPa and 875 hPa and COT between 5.8 and 9.4 (as indicated by a yellow square in (a)); (c) As in (b) but for clouds with CTP between 180 hPa and 245 hPa and COT between 2.2 and 3.6 (as indicated by a red square in (a)).*

5 References

Hahn, C.J., W.B. Rossow and S.G. Warren, 2001: ISCCP Cloud Properties Associated with Standard Cloud Types Identified in Individual Surface Observations, J. Clim., 14, 11-28.

Lin, W.Y. and M.H Zhang, 2004: Evaluation of clouds and their radiative effects simulated by the NCAR Community Atmospheric Model against satellite observations. J. Climate, 17, 3302-3318.

Marchand, R., T. Ackerman, M. Smythe, and W.B. Rossow, 2010: A review of cloud top height and optical depth histograms from MISR, ISCCP and MODIS. J. Geophys. Res., 115, D16206, doi:10.1029/2009JD013422.

Oreopoulos, L., and W. B. Rossow. 2011. "The cloud radiative effects of International Satellite Cloud Climatology Project weather states." J. Geophys. Res. 116 (D12): D12202 [10.1029/2010JD015472]

Pincus, R., S. Platnick, S. A. Ackerman, R. S. Hemler, and R. J. P. Hofmann, 2012: Reconciling simulated and observed views of clouds: MODIS, ISCCP, and the limits of instrument simulators. J. Climate, 25, 4699-4720. doi:10.1175/JCLI-D-11-00267.1.

Rossow, W.B. and R.A. Schiffer, 1991: ISCCP Cloud Data Products, Bull. Amer. Meteorol. Soc., 72, 1, 2-20.

Rossow, W.B. and R.A. Schiffer, 1999: Advances in Understanding Clouds from ISCCP, Bull. Amer. Meteorol. Soc., 80, 11, 2261-2287.

Rossow, W.B., G. Tselioudis, A. Polak, and C. Jakob, 2005: Tropical climate described as a distribution of weather states indicated by distinct mesoscale cloud property mixtures. Geophys. Res. Lett., 32, L21812, doi:10.1029/2005GL024584.

Shupe, M.D., P. Kollias, P.O.G. Persson and G.M. McFarquhar, 2008: Vertical Motions in Arctic Mixed-Phase Stratiform Clouds, J. Atmos. Sci., 65, 1304-1322.

Zelinka, M. D., S. A. Klein, and D. L. Hartmann, 2012: Computing and Partitioning Cloud Feedbacks Using Cloud Property Histograms. Part I: Cloud Radiative Kernels. J. Climate, 25, 3715–3735. doi:10.1175/JCLI-D-11-00248.1.

Zelinka, M. D., S. A. Klein, and D. L. Hartmann, 2012: Computing and Partitioning Cloud Feedbacks Using Cloud Property Histograms. Part II: Attribution to Changes in Cloud Amount, Altitude, and Optical Depth. J. Climate, 25, 3736–3754. doi:10.1175/JCLI-D-11-00249.1.

Zhang, M.H., W.Y. Lin, S.A. Klein, J.T. Bacmeister, S. Bony, R.T. Cederwall, A.D. Genio, Del J.J. Hack, N.G. Loeb, U. Lohmann, P. Minnis, I. Musat, R. Pincus, P. Stier, M.J. Suarez, M.J. Webb, J.B. Wu, S.C. Xie, M.S. Yao, J.H. Zhang, 2005: Comparing clouds and their seasonal variations in 10 atmospheric general circulation models with satellite measurements. J. Geoph. Res., 110, D15, D15S02.